Title

Correlating steric hydration forces with water dynamics through surface force and diffusion NMR measurements in a lipid–DMSO–H2O system

Journal

Proceedings of the National Academy of Sciences of the United States of America, 112(34)

ISSN

0027-8424

Authors

Schrader, Alex M
Donaldson, Stephen H
Song, Jinsuk
et al.

Publication Date

2015-08-25

DOI

10.1073/pnas.1512325112

Correlating steric hydration forces with water dynamics through surface force and diffusion NMR measurements in a lipid–DMSO–H_2O system

Alex M. Schrader[a], Stephen H. Donaldson Jr.[a], Jinsuk Song[b], Chi-Yuan Cheng[b], Dong Woog Lee[a], Songi Han[a,b], and Jacob N. Israelachvili[a,c,1]

[a]Department of Chemical Engineering, University of California, Santa Barbara, CA 93106-5080; [b]Department of Chemistry and Biochemistry, University of California, Santa Barbara, CA 93106-5050; and [c]Materials Department, University of California, Santa Barbara, CA 93106-5050

Contributed by Jacob N. Israelachvili, June 27, 2015 (sent for review February 13, 2015)

Dimethyl sulfoxide (DMSO) is a common solvent and biological additive possessing well-known utility in cellular cryoprotection and lipid membrane permeabilization, but the governing mechanisms at membrane interfaces remain poorly understood. Many studies have focused on DMSO–lipid interactions and the subsequent effects on membrane-phase behavior, but explanations often rely on qualitative notions of DMSO-induced dehydration of lipid head groups. In this work, surface forces measurements between gel-phase dipalmitoylphosphatidylcholine membranes in DMSO–water mixtures quantify the hydration- and solvation-length scales with angstrom resolution as a function of DMSO concentration from 0 mol% to 20 mol%. DMSO causes a drastic decrease in the range of the steric hydration repulsion, leading to an increase in adhesion at a much-reduced intermembrane distance. Pulsed field gradient NMR of the phosphatidylcholine (PC) head group analogs, dimethyl phosphate and tetramethylammonium ions, shows that the ion hydrodynamic radius decreases with increasing DMSO concentration up to 10 mol% DMSO. The complementary measurements indicate that, at concentrations below 10 mol%, the primary effect of DMSO is to decrease the solvated volume of the PC head group and that, from 10 mol% to 20 mol%, DMSO acts to gradually collapse head groups down onto the surface and suppress their thermal motion. This work shows a connection between surface forces, head group conformation and dynamics, and surface water diffusion, with important implications for soft matter and colloidal systems.

dimethyl sulfoxide | hydration shell | membrane interactions | lipid solvation | hydrodynamic radius

Solute additives (e.g., osmolytes or denaturants) often play a key role in modulating biological interactions, where molecules can recognize each other and form assemblies. Dimethyl sulfoxide [DMSO, $(O = S)(CH_3)_2$] and DMSO–water mixtures in particular have attracted particular interest in biology and chemistry. DMSO is one of the most commonly used cryoprotectants in cellular systems (1), where it colligatively reduces the melting point of aqueous solutions and exerts additional effects that prevent cellular damage on freezing/vitrification. Additional effects not seen with conventional glycol- and saccharide-based cryoprotectants include an increase in lipid membrane permeability of an array of solutes (2), promotion of cell fusion (3) and differentiation (4), and enhanced membrane resealing after damage (5). These phenomena are well-documented along with their dependence on DMSO concentration, but the molecular behavior of DMSO near lipid membranes remains a mystery.

Bulk properties of DMSO–water mixtures are well-characterized. The oxygen and sulfur atoms of DMSO have a partial negative and positive charge, respectively, giving rise to a dipole moment of 3.96 Debye that exceeds nearly all conventional solvents. Dielectric relaxation spectroscopy (6), molecular dynamics simulations (7), and ^{1}H NMR studies (8) have shown that bulk water forms hydrogen bonds with the oxygen of DMSO in the ratio of 1:2 (DMSO:water), bonds that are approximately five times longer lived than water–water hydrogen bonds (7). Consequently, DMSO–water mixtures near this 1:2 ratio display maxima or minima in density (9), viscosity (9), freezing point (10), and heat of mixing (11) among other properties (8). However, any experimental quantification of the properties of DMSO–water bonds at the lipid membrane surface (let alone as a function of DMSO concentration) remains unknown.

Previous work has primarily focused on DMSO–lipid interactions and the subsequent effects on thermotropic lipid-phase behavior, typically involving the most biologically prevalent class of lipid: phosphatidylcholine (PC). IR spectroscopy experiments (12) have suggested that the partially charged atoms of DMSO associate with oppositely charged moieties of gel-phase dipalmitoylphosphatidylcholine (DPPC) lipid head groups, potentially replacing water–lipid hydrogen bonds. Differential scanning calorimetry studies have found DMSO to monotonically increase the chain melting temperature (T_m) of DPPC lamellae (13). Concentrations of DMSO above 10 mol% (1 DMSO molecule per 9 water molecules) at 25 °C induce a subgel phase (14), which is characterized by different head group ordering. Small-angle X-ray and neutron scattering studies (15–17) have shown that DMSO substantially decreases the solvent gap thickness (equilibrium separation) between lamellae of both gel-phase and fluid PC multilamellar vesicles. Explanations for the phase behavior and equilibrium separation phenomena often implicate some mechanism of head group dehydration/desolvation brought about by DMSO (14, 16, 18).

Recent measurements of translational water diffusivity within ~1 nm of the surface of unilamellar DPPC (gel phase) and

Significance

We use the common biological additive DMSO to show quantitatively the impact that surface-bound water has on interactions between lipid bilayers, the membranes that separate the interior of cells from the surroundings. We present a number of metrics to gauge the hydration of the bilayer surfaces and show how the metrics are affected by the concentration of DMSO in the solvent. This work further connects measurements of surface forces, surface structure and dynamics, and surface water diffusion with significant and broad implications for soft matter systems.

Author contributions: A.M.S., S.H.D., J.S., C.-Y.C., S.H., and J.N.I. designed research; A.M.S. and S.H.D. performed research; A.M.S. and S.H.D. contributed new reagents/analytic tools; A.M.S., S.H.D., J.S., D.W.L., S.H., and J.N.I. analyzed data; and A.M.S., S.H.D., S.H., and J.N.I. wrote the paper.

The authors declare no conflict of interest.

[1]To whom correspondence should be addressed. Email: jacob@engineering.ucsb.edu.

This article contains supporting information online at www.pnas.org/lookup/suppl/doi:10.1073/pnas.1512325112/-/DCSupplemental.

dioleoylphosphatidylcholine (DOPC, fluid phase) vesicles using the Overhauser Dynamic Nuclear Polarization relaxometry technique (19) show a continual increase in water diffusivity with DMSO concentration (20). Water diffusivity, D_w, near the head groups increased ~50% in going from 0 mol% DMSO (pure water; $D_w = 7.7 \times 10^{-10}$ m^2/s) to 7.5 mol% DMSO ($D_w = 11.4 \times 10^{-10}$ m^2/s) for DPPC membranes, whereas the mobility and ordering of PC head groups remained constant up to 10 mol% (20). This hydration dynamics study is perhaps the strongest evidence yet of DMSO weakening the cohesion of the surface water, which suggests that head group dehydration is facilitated at DMSO concentrations <10 mol%. Although plausible, no rigorous connection has been experimentally established between solvent dynamics and the forces that govern membrane fusion, permeability, or the equilibrium separation of bilayers in multilamellar lipid membrane systems.

Using the surface forces apparatus (SFA) technique, the force–distance measurements between supported DPPC bilayers presented in this work offer a quantitative description of the effect of DMSO on lipid solvation-length scales. We restrict ourselves to DMSO concentrations <20 mol%, which many of the aforementioned literature studies have done. A pulsed field gradient (PFG) NMR study of molecular diffusion and SFA measurement showing hydration of the choline moiety provide independent support of the quantifications made from fitting the interbilayer forces. Short-range forces (at surface separations <2 nm) are especially informative and sensitive to the DMSO concentration, acting at distances where one would expect effects on membrane rigidity, head group ordering, and solvent structure to manifest themselves. The role of water in short-range bilayer interactions has been a point of contention (21–23), especially in explaining the pseudoexponential repulsion commonly observed below ~2 nm of separation. It has been argued that solvent-structural "hydration forces" govern this repulsion (24) and conversely, that entropic fluctuations of thermally mobile head groups dominate the interaction (25). Through modulating the solvation of lipid head groups with DMSO, this study provides direct insight into addressing this fundamental question of the existence and origin of hydration forces.

Results and Analysis

Equilibrium Force–Distance Measurements. To determine the effects of the additive DMSO on the lipid bilayer interactions, the interaction forces were measured with SFA. Briefly, in SFA experiments, the absolute distance between back-silvered mica surfaces in a cross-cylinder geometry is measured with interferometry, and the force, F, is measured by the deflection of a cantilever spring (26). Force–distance profiles are typically shown as the force, F, normalized by the radius of the surfaces, R, plotted against the separation distance, D (i.e., F/R vs. D). Force is converted to the interaction energy between flat plates, W, using the Derjaguin Approximation, $W = F/2\pi R$ (27) (valid for weak adhesion, which is the case in this work). Before each experiment, the mica sheet thicknesses are measured followed by Langmuir–Blodgett deposition of bilayers as described in *Materials and Methods*.

The zero distance, $D = 0$, corresponds to the hypothetical bilayer–bilayer contact in air—a convention often used in SFA and osmotic stress measurements between bilayers (24, 28). Thermal fluctuations of the head groups and their associated hydration in water prevent the surfaces from approaching $D = 0$ in practice. The single-bilayer anhydrous thickness, T_o, was found to be 5.0 ± 0.1 nm (the procedure is described in *Materials and Methods*).

Representative force–distance profiles, F/R vs. D, for DMSO concentrations, C_{DMSO}, between 0 mol% and 20 mol% are shown in Fig. 1. Quasistatic force measurements were taken in the repulsive regime (Fig. 1*A*) using a piezoelectric crystal to

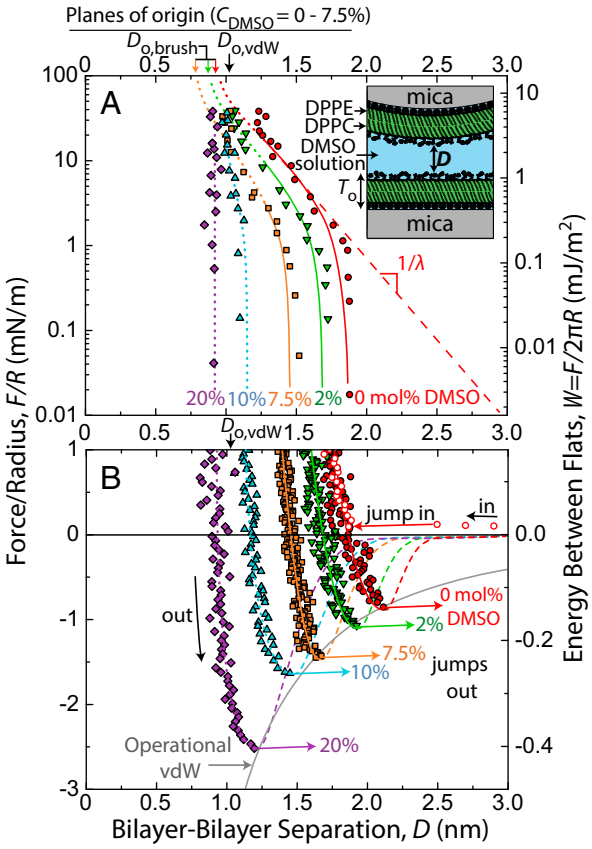

Fig. 1. Forces, F, measured between mica-supported gel-phase DPPC bilayers in DMSO–water mixtures at 22 °C and pH 6.0 ± 0.2. Solid colored lines corresponding to 0 mol%, 2 mol%, and 7.5 mol% DMSO runs are fits comprised of polymer brush and van der Waals forces. Force curves for 10% and 20% DMSO were unable to be fitted with the polymer brush equation owing to their steepness in the repulsive regime, but corresponding hand-drawn (dotted) lines were included for consistency. (*A*) Static measurements of repulsive forces on a semilog plot. Values for the fits at D < 1.3 nm were drawn by hand (dotted) because of mathematical divergence of the van der Waals force near $D_{o,vdw}$. The steep upturns of forces above 20 mN/m in the 0–7.5 mol% data series occurred when the surfaces began deforming noticeably, resulting in inaccurate R values. (*B*) Adhesion forces, F_{ad}, measured on slow separation of the surfaces. Dashed lines show a reduced van der Waals force resulting from screening of the Hamaker constant by the zwitterionic head groups (28). The solid gray line corresponds to a van der Waals force ($D_{o,vdw}$ = 0 nm, $A = 2.3 \times 10^{-20}$ J), which may be operationally used to describe adhesion forces in this system but was not used in the full fits of the force curves.

move one surface in steps of 2–20 nm, with subsequent 30 s of equilibration time before the separation distance, D, was measured. In the attractive regime (Fig. 1*B*), measurements were made dynamically but very slowly, wherein one surface was driven at a constant speed (0.1–0.2 nm/s). Values for the adhesive force, F_{ad}/R, are given by the depth of forces into the attractive regime before the jump out, a mechanical instability dependent on spring stiffness. Dynamic measurements allowed for more accurate determination of adhesive force, F_{ad}/R (±0.1 mN/m), and the corresponding separation distance at which the jump out occurs at D_o (±0.1 nm) on separation of the surfaces.

Adhesive forces/energies increased monotonically with C_{DMSO}, and the value at C_{DMSO} = 20 mol% (F_{ad}/R = –2.6 mN/m, W_{ad} = –0.41 mJ/m^2) was approximately three times that in water (F_{ad}/R = –0.9 mN/m, W_{ad} = –0.14 mJ/m^2). The separation where the adhesive force is measured, D_o, corresponds to the equilibrium separation (i.e., the energy minimum) between flat plates by way of the Derjaguin Approximation. D_o decreased monotonically with

C_{DMSO}. Explanations for these trends are given in *Discussion and Conclusions*. The equilibrium water gap thickness between lamellae of gel-phase multilamellar vesicles has been measured as a function of DMSO concentration by using small-angle neutron scattering (15), with quantitative values comparable with our D_o values (Fig. S1).

Forces between bilayers in DMSO–water mixtures have been measured one time before (29). SFA measurements of DOPC bilayers in a 10 mol% DMSO solution showed that F_{ad}/R approximately doubled in going from 0 mol% to 10 mol% DMSO, which is in agreement with our measurements. Because the measurements were done on fluid-phase bilayers, additional effects, such as bilayer fusion and nonreversible structural disruption, were observed that do not appear in our gel-phase measurements.

Fitting Models for Force Curves. The measured force–distance profiles for $C_{DMSO} \leq 7.5$ mol% can be fitted with a high degree of accuracy in the range 1.3 nm $< D <$ 2.2 nm using two components of force, an attractive van der Waals force, and a repulsive hydrated head group overlap (polymer brush) force. The van der Waals equation is as follows (Eq. **1**):

$$\frac{F(D)}{R} = \frac{-A}{6\left(D - D_{o,vdw}\right)^2}, \qquad [1]$$

where A is the Hamaker constant, which can be fitted and also calculated from the dielectric constant and refractive index of the bilayers and solution, and $D_{o,vdw}$ is the plane of origin from which the force effectively originates owing to the head groups that protrude ~0.5 nm out from the anhydrous thickness, $D = 0$, of each bilayer. The head group overlap force contribution, slightly modified to account for hydration-excluded volume effects, is as follows (Eq. **2**) (30):

$$\frac{F(D)}{R} = \frac{16\pi kTL}{35s^3}\left[7\left(\frac{2L}{D - D_{o,brush}}\right)^{5/4} + 5\left(\frac{D - D_{o,brush}}{2L}\right)^{7/4} - 12\right] \qquad [2]$$

over the range $D_{o,brush} < D < D_{o,brush} + 2L$, where $D_{o,brush}$ is the plane of origin of the force, L is the height of the hydrated head group brush, and s is the lateral separation between head groups. Hydration effects are often not explicitly accounted for, because typical brush heights greatly exceed solvent dimensions. The $D_{o,brush}$ term is included here to account for such effects, analogous to the van der Waals excluded volume correction to the pressure of a gas; V^{-1} becomes $[V(1 - b/V)]^{-1}$, which is used to calculate finite ion sizes in surface forces measurements (27). Fitting parameters and associated SDs used in Eqs. **1** and **2** are shown in Table 1. For $D/2L$ in the range 0.2–0.9, Eq. **2** is roughly exponential, with a decay length $\lambda = L/\pi$. Fits using this exponential approximation are given in Fig. S3 and Table S1. At concentrations $C_{DMSO} \geq 10$ mol%, the repulsive force was too steep to obtain an accurate value of λ or L.

For all of the data series corresponding to $C_{DMSO} \leq 7.5$ mol% in Fig. 1, forces at $D < 1.3$ nm were not fitted, and thus, the fits in this range are drawn by hand. At separations $D < 1.3$ nm, the sum of Eqs. **1** (for van der Waals) and **2** (for head group overlap) begins to diverge strongly toward negative values of F because of the D^{-2} dependence of the van der Waals contribution. This divergence has never been observed experimentally, likely because of a reduction in $D_{o,vdw}$ on compression of the bilayers. Forces on approach at separations $D > D_o$ (shown only for $C_{DMSO} = 0\%$) were not fitted with Eq. **1** or Eq. **2** but likely contain contributions from the van der Waals force reduced by a factor of ~6 because of screening of the zero-frequency contribution of A by the zwitterionic head groups (28) and a weak electrostatic repulsion. The electrostatic repulsion is caused by either a residual potential from the mica surface (corresponding to a surface potential $\psi \sim 30$ mV) or traces of charged lipid impurities in the bilayer ($\psi \sim 20$ mV). The latter has been observed several times previously (31, 32).

At $C_{DMSO} \leq 7.5$ mol%, fitted and theoretical values of A are in good agreement with each other using a constant van der Waals plane of origin, $D_{o,vdw} = 1.05$ nm (28). The discrepancy at $C_{DMSO} \geq 10$ mol% could be caused by a large difference in the dielectric properties between the interfacial and bulk solvent, but one might expect this difference to exist at the lower DMSO concentrations as well. Alternatively, a slight reduction of $D_{o,vdw}$ for $C_{DMSO} \geq 10$ mol% would rationalize the difference. The values for $D_{o,vdw}$, which make the fitted and theoretical A values match, are, for 10, 15, and 20 mol% DMSO, 0.9 ± 0.1, 0.9 ± 0.1, and 0.7 ± 0.1 nm, respectively. These values for A correspond physically to a change in head group conformation, resulting in $D_{o,vdw}$ for each bilayer shifting ~0.1 nm inward toward the respective hydrocarbon regions relative to $D_{o,vdw}$ in $C_{DMSO} < 7.5$ mol% solutions.

The adhesive force between the bilayers increases monotonically with C_{DMSO}, despite a monotonically decreasing value of A (shown in Table 1), which indicates that the increased attraction is caused by a decreased range of the repulsive force. A similar conclusion was reached by Claesson et al. (33) in measurements of forces between poly(ethylene oxide) (PEO) monolayers in water. With an increase in temperature, Claesson et al. (33) observed an increase in adhesion and a decrease in D_o, which were shown to be a result of a decreased range of the steric hydration force caused by dehydration of PEO groups rather than

Table 1. Parameters for head group overlap (Eq. 2) and Van der Waals (Eq. 1) fits

Mol% DMSO	Brush length,* L (±0.03 nm)	Lateral head group separation, s (±0.1 nm)	Plane of origin, $D_{o,brush}$ (±0.1 nm)	Hamaker constant, A ($\times 10^{-21}$ J)	
				Fitted,† ±0.4	Theoretical‡
0	0.64	1.4	0.9	7.0	7.0
2	0.57	1.3	0.9	6.2	6.4
5	0.53	1.2	0.8	5.1	5.4
7.5	0.47	1.1	0.8	4.3	4.9
10	§	§	§	2.6	4.4
15	§	§	§	2.3	3.7
20	§	§	§	0.8	3.2

*Corresponding decay lengths (λ; ±0.01 nm) in the exponential regions are 0.20, 0.18, 0.17, and 0.15 nm, respectively.
†Fitted A values were calculated using a constant $D_{o,vdw}$ of 1.05 nm (28).
‡Theoretical values for A calculated using values of dielectric constant ($\varepsilon_1 = 3.8$) and refractive index ($n_1 = 1.464$) for bilayers and bulk values of ε_3 and n_3 for the solvent (9) (Fig. S2).
§Meaningful fitting parameters could not be obtained because of the steepness of the force in the repulsive regimes.

augmentation of the attractive van der Waals force. In this work, at $C_{DMSO} < 10$ mol%, values for L and $D_{o,brush}$ decreased with increasing C_{DMSO}, suggesting either a gradual collapse of the head groups or more likely, a gradual decrease in head group hydrated excluded volume, which is addressed in *Discussion and Conclusions*. The fitted head group separation, s, decreased slightly as well but always exceeded the predetermined value of 0.72 nm according to head group density. Even in grafted polymer brush systems, fitted values of s are known to vary from actual values for a number of reasons (25, 30, 34). In this case, the effect of lateral diffusion of head groups and their short length compared with the typical polymer brush make the trend in s difficult to interpret physically.

It is worth noting the other potential contributions to short-range bilayer interaction that are often considered but do not seem to be of significance in our results. Four main contributions to the steric hydration repulsion between bilayers have been identified in the literature (25): undulation (Helfrich), protrusion, peristaltic (bilayer compression), and head group overlap. The entropic nature of these forces allows one to include hydration-excluded volume effects through shifts in planes of origin without the addition of a separate hydration force. The undulation force arises from the suppression of long-wavelength thermal ripples in the free-standing membranes on surface approach and can be ruled out in measurements between supported bilayers, which is the case in this work. The protrusion force arises from suppression of molecular-scale protrusions of lipids into the solution. It is approximately exponential at $D > 1.1$ nm, and the decay length is inversely proportional to the interfacial energy of the solvent–hydrocarbon interface (25). This interfacial energy, however, decreases monotonically with DMSO concentration (Fig. S4), a trend that would dictate a longer decay length with increasing DMSO concentration, and therefore, changes in the protrusion force alone cannot explain the presented trends. Bilayer compressibility is not explicitly known as a function of DMSO concentration, but in pure water, McIntosh and Simon (35) found through X-ray diffraction that gel-phase DPPC bilayer thickness does not change by more than 3% on approach to 0.2-nm separation. Moreover, Marra and Israelachvili (28) found only a 0.1-nm decrease in the thickness of fluid-phase egg PC bilayers on compressing to $F/R > 20$ mN/m ($D = 0.9$ nm) in water through refractive index measurements. Therefore, contributions from the peristaltic force are also neglected. Thus, head group overlap is left as the primary contributor to the repulsive force.

With such large DMSO concentrations, one might expect significant contributions from a depletion force in our measurements, but we believe that this is not the case. DMSO depletion would dictate adhesive forces ~100 times larger than those observed experimentally. Additional reasoning is given in *SI Text*, section S5.

Regardless of the fitting equation(s) used, the trend of the repulsive forces becoming shorter-ranged with added DMSO is apparent, and semiquantitative statements about the role of hydration forces can be made. For example, looking at Fig. 1*A* and Fig. S5 for more detail, one could say that, at $F/R \sim 20$ mN/m, the interaction force in 0% solution is shifted ~0.1 nm outward (to higher D values) per bilayer more than that in 7.5 mol% solution, despite a difference of 0.2–0.3 nm in extension of the uncompressed and fully hydrated head groups into solution (based on D_o values), suggesting that approximately one layer of bound/hydration water is removed from the interfacial region in 0% DMSO solution on compression to 20 mN/m. The presented method of analysis offers a number of parameters that aid in physical interpretation: L, $D_{o,brush}$, and fitted A (or shifts in $D_{o,vdw}$), but it is difficult to definitively conclude from SFA measurements alone how much DMSO affects the hydrated excluded volume of the head groups, whereas it is clear that DMSO reduces the interbilayer repulsion.

NMR Measurements of Phosphate and Tetramethylammonium Hydrodynamic Radius. PFG NMR is a well-established technique to measure bulk solute diffusivity averaged over milliseconds to seconds observation times, from which an effective hydrated solute size, time-averaged over the applied observation window, can be extracted (36). The effect of DMSO on the solvated radius of the lipid head group was examined by diffusion NMR measurements on model PC head group moieties in bulk solution: dimethyl phosphate (DMP^-) and tetramethylammonium (TMA^+) molecules. The measured solvent viscosities (Table S2) and solute diffusivities were used to calculate the solute hydrodynamic radius, r_H, using the Stokes–Einstein equation (*Materials and Methods*). Fig. 2 shows solute r_H at values of C_{DMSO}, where the SFA measurements were conducted.

Values of r_H steadily decreased for both ions up to $C_{DMSO} = 7.5$ mol%, after which point values remained constant within error. The decrease in DMP^- solvated volume was 0.1 nm^3 in going from $C_{DMSO} = 0$ mol% to 10 mol%, perhaps corresponding to an equivalent shedding of approximately seven water molecules from the solvation shell. The decrease in TMA^+ solvated volume was 0.04 nm^3 over the same range of C_{DMSO}, which corresponds to approximately three water molecules. The diffusion NMR measurements, although not quantitatively transferable to SFA fitting parameters, show a solvation contribution to the decreased range of the repulsion observed in SFA measurements on increasing C_{DMSO} from 0 mol% to 7.5 mol%.

In addition to bulk NMR measurements, SFA measurements between mica surfaces (without lipids) in aqueous salt solutions can give clear information about cation hydration. Cations adsorb to the negatively charged mica surfaces, and upon bringing the surfaces together, dehydration of the adsorbed cations gives rise to a repulsive hydration force—the magnitude and range of which are larger for more hydrated cations (37). SFA measurements between mica surfaces in ternary mixtures of water, DMSO, and TMACl are shown in Fig. S6. The results show a decreased range of the hydration force in going from 0 mol% to 10 mol% DMSO and little effect beyond, which corroborates the trend in r_H values for TMA^+ measured with NMR.

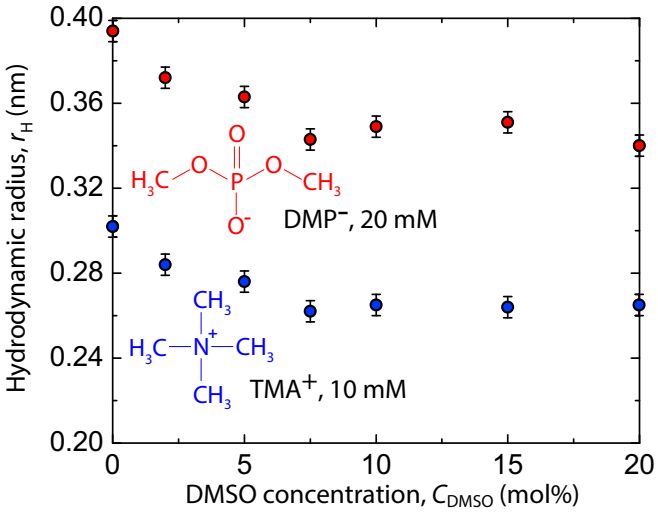

Fig. 2. Hydrodynamic radii, r_H, of DMP^- and TMA^+ as calculated from bulk NMR diffusion measurements in DMSO-d_6–D_2O–salt mixtures at 25 °C. Measurements were made on solutions containing 20 mM NaDMP (~0.05 mol%) and 10 mM TMACl (~0.025 mol%).

Discussion and Conclusions

The SFA and NMR measurements described above, in addition to literature observations, suggest two regimes of DMSO interaction with the PC head group. The first regime, illustrated in Fig. 3*B* (C_{DMSO} = 2–7.5 mol%), is partly characterized by unchanging head group ordering and dynamics according to ^{31}P NMR anisotropy measurements and the electron paramagnetic resonance (EPR) line shape of nitroxide spin probes tethered to the PC group (20). Scattering studies in the literature, although relatively insensitive to choline position, have also shown no indication of a change in head group conformation over this concentration range (14). Based on this knowledge, the presented SFA and NMR measurements show a gradual decrease in the solvated size of the PC head group that occurs in this regime of DMSO concentration. The decrease in L and $D_{o,brush}$ observed in the SFA measurements may have a small contribution from a gradual collapse of the head groups but is mostly caused by a decrease in PC head group-excluded volume because of its desolvation. It follows that the decreasing range of the repulsion between bilayers shown in this work in going from 0 to 7.5 mol% DMSO is a desolvation effect.

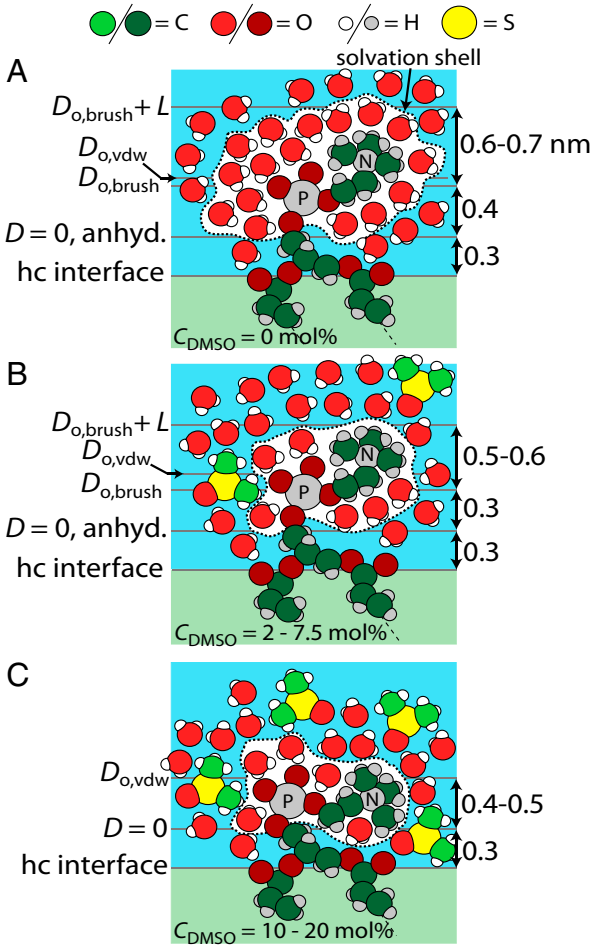

Fig. 3. Schematic views of the PC head group in DMSO–water mixtures with various dimensions and planes of origin drawn to scale in (*A*) pure water, (*B*) 2–7.5 mol% DMSO, and (*C*) 10–20 mol% DMSO. Atoms labeled P and N represent phosphorous and nitrogen, respectively. The hydrocarbon/head group interface labeled "hc interface" is drawn at the height of the carbonyl groups. The van der Waals plane of origin, $D_{o,vdw}$, is located at the same height in *A* and *B*, because the position of the choline is relatively unchanged between the two scenarios. Brush length, L, and brush plane of origin, $D_{o,brush}$, are smaller in *B* than in *A* because of a decrease in head group-excluded volume (i.e., dehydration). $D_{o,vdw}$ is smaller in *C* than in *B*, reflecting gradual collapse of the choline at large DMSO concentrations and orientation of the P-N vector parallel with the plane of the bilayer. In *C*, the corresponding bilayer displays little to no polymer brush character in SFA measurements.

In the second regime, illustrated in Fig. 3*C* (C_{DMSO} = 10–20 mol%), head groups are gradually collapsed down onto the surface, and their mobility suppressed, which is, once again, corroborated by the EPR and NMR measurements in ref. 20. The repulsive force in Fig. 1*A* rises steeply and can no longer be described by Eq. **2** for brushes. The van der Waals plane of origin, $D_{o,vdw}$, subsequently shifts inward ~0.1 nm for each bilayer. However, the NMR measurements suggest that the solvated radius remains constant within this regime, indicating that the mobility of the head groups is suppressed while they remain solvated to a similar degree.

Although our measurements cannot directly probe the placement and conformation of DMSO around the head groups, we can deduce that DMSO must not be strongly bound to either the phosphate or choline. If the DMSO molecule, approximately a sphere with a diameter of 0.58 nm (38), were to bind strongly and replace water tightly bound to the charged moieties of the head group, one would expect the hydrodynamic radius (as probed by NMR) and excluded volume to increase. Rather, the DMSO competes with the PC head group for hydrogen bonds and favorable electrostatic interactions with water. Recalling that water–DMSO hydrogen bonds are stronger than water–water hydrogen bonds (7), it follows that such competition tends to draw bound water out of its strongly oriented and tightly bound state. The driving force for the change in head group conformation above 10 mol% DMSO is unclear, but based on the SFA fitting parameters, we propose that DMSO gradually collapses the PC head group and thus, decreases the angle between the membrane plane and P-N vector as illustrated in Fig. 3*C*. Perhaps the DMSO dehydrates the carbonyl or glycerol portions of the lipid in this regime, allowing for collapse of the head group. It should be noted that the above mechanisms are not general to all cryoprotectants or polar cosolvents, which is shown in a control experiment using glycerol instead of DMSO (Fig. S7).

By concluding that the shortening of the range of the repulsive force in going from 0 mol% to 7.5 mol% DMSO is primarily a solvation effect, we infer that the role of water in lipid membrane interactions is to extend the range and decay length of the interaction, a conclusion reached several times previously by experimental and theoretical methods (22, 25, 39). This extension is generally not referred to as a separate hydration force, but rather as an excluded volume correction to a steric force. Hydration force is typically used to describe forces wherein surface-bound water is removed on compression (i.e., a shrinking head group-excluded volume on compression), giving rise to a characteristic exponential decay length of 0.3–1.0 nm (37). Fitting our data with an additional exponential hydration force (in addition to Eqs. **1** and **2**) results in poorer fits than those shown in Fig. 1, regardless of the fitting parameters. However, replacing Eq. **2** (head group overlap) with an exponential force yields acceptable results (Fig. S3). As mentioned above, it does appear that a small amount of bound water is evicted on compression. The true role of water remains a subtle one, but nonetheless seems to be captured in our fitting model.

The acknowledgment of a solvation contribution to measured forces allows for comparison with interfacial solvent properties and in particular, water diffusivity. We see now that the monotonically increasing vesicle surface water diffusivity in going from 0 mol% to 7.5 mol% DMSO, as measured in ref. 20, coincides with a decreased range of repulsive forces and subsequently greater adhesion. DMSO weakens water binding to the head groups, which causes the interfacial water to diffuse faster (more like water diffuses in the bulk) and a shortened range of the repulsive force through a decrease in hydrated excluded volume. Quantitatively establishing a correlation between surface or head group water

diffusivity and surface forces would require overcoming the hurdles of rigorous thermodynamic and/or kinetic treatment. Our results reveal the potential for such a correlation, which could be useful in using local water diffusivity as a predictive tool for the stability of colloids and complex fluid systems.

Materials and Methods

Before each SFA experiment, the two mica surfaces were brought into contact in air to calibrate the absolute zero of separation distance. Next, the mica surfaces were coated with the lipid bilayers using Langmuir–Blodgett deposition and transferred under water to the SFA. The bilayers in the SFA experiments were composed of an inner leaflet monolayer of dipalmitoylphosphatidylethanolamine (DPPE, deposited at 28 mN/m surface pressure, 0.42 nm^2 per lipid) and an outer leaflet monolayer of DPPC (19 mN/m, 0.52 nm^2). The single-bilayer thickness, T_o, was calculated from SFA measurements of the thickness of two DPPE monolayers in air and two DPPC monolayers in air both at the same surface pressure as the bilayers in the force measurements.

The salt NaDMP was synthesized from trimethylphosphate and sodium iodide as previously reported (40) and confirmed to have ~96% purity by NMR. NMR diffusion measurements were done using a PFG One-Shot Experiment (Doneshot; Varian), for which a detailed explanation can be found in ref. 41. Hydrodynamic radii were calculated using a modified Stokes–Einstein equation for scenarios when solute size is comparable with solvent size (42). Viscosity measurements were done using a Lovis 2000 M Anton Parr Viscometer with a 1.59-mm (400 μL) glass capillary tube and stainless steel ball. Interfacial tension measurements were made using a Wilhelmy plate. The following materials were purchased from commercial suppliers and used without additional purification: DPPC, DPPE, DMSO, DMSO-d_6, D_2O, and TMACl.

ACKNOWLEDGMENTS. We thank M. E. Helgeson and J. Kim for assistance in the viscosity measurements. This work was supported by Materials Research Science and Engineering Centers (MRSEC) Program of the National Science Foundation Award DMR 1121053.

1. Lovelock JE, Bishop MWH (1959) Prevention of freezing damage to living cells by dimethyl sulphoxide. *Nature* 183(4672):1394–1395.
2. Anchordoguy TJ, Carpenter JF, Crowe JH, Crowe LM (1992) Temperature-dependent perturbation of phospholipid bilayers by dimethylsulfoxide. *Biochim Biophys Acta* 1104(1):117–122.
3. Ahkong QF, Fisher D, Tampion W, Lucy JA (1975) Mechanisms of cell fusion. *Nature* 253(5488):194–195.
4. Lyman GH, Preisler HD, Papahadjopoulos D (1976) Membrane action of DMSO and other chemical inducers of Friend leukaemic cell differentiation. *Nature* 262(5567): 361–363.
5. Shi R, Qiao X, Emerson N, Malcom A (2001) Dimethylsulfoxide enhances CNS neuronal plasma membrane resealing after injury in low temperature or low calcium. *J Neurocytol* 30(9-10):829–839.
6. Lu Z, Manias E, Macdonald DD, Lanagan M (2009) Dielectric relaxation in dimethyl sulfoxide/water mixtures studied by microwave dielectric relaxation spectroscopy. *J Phys Chem A* 113(44):12207–12214.
7. Luzar A, Chandler D (1993) Structure and hydrogen bond dynamics of water–dimethyl sulfoxide mixtures by computer simulations. *J Chem Phys* 98(10):8160–8173.
8. Baker ES, Jonas J (1985) Transport and relaxation properties of dimethyl sulfoxide-water mixtures at high pressure. *J Phys Chem* 89(9):1730–1735.
9. LeBel RG, Goring DAI (1962) Density, viscosity, refractive index, and hygroscopicity of mixtures of water and dimethyl sulfoxide. *J Chem Eng Data* 7(1):100–101.
10. Havemeyer RN (1966) Freezing point curve of dimethyl sulfoxide–water solutions. *J Pharm Sci* 55(8):851–853.
11. Fox MF, Whittingham KP (1975) Component interactions in aqueous dimethyl sulphoxide. *J Chem Soc Faraday Trans 1* 71:1407–1412.
12. Shashkov SN, Kiselev MA, Tioutiounnikov SN, Kiselev AM, Lesieur P (1999) The study of DMSO/water and DPPC/DMSO/water system by means of the X-ray, neutron small-angle scattering, calorimetry and IR spectroscopy. *Physica B Condens Matter* 271(1-4): 184–191.
13. Yu ZW, Quinn PJ (1995) Phase stability of phosphatidylcholines in dimethylsulfoxide solutions. *Biophys J* 69(4):1456–1463.
14. Tristram-Nagle S, Moore T, Petrache HI, Nagle JF (1998) DMSO produces a new subgel phase in DPPC: DSC and X-ray diffraction study. *Biochim Biophys Acta* 1369(1):19–33.
15. Gorshkova JE, Gordeliy VI (2007) Investigation of the interaction of dimethyl sulfoxide with lipid membranes by small-angle neutron scattering. *Crystallography Reports* 52(3):535–539.
16. Kiselev MA, Lesieur P, Kisselev AM, Grabielle-Madelmond C, Ollivon M (1999) DMSO-induced dehydration of DPPC membranes studied by X-ray diffraction, small-angle neutron scattering, and calorimetry. *J Alloys Compd* 286(1-2):195–202.
17. Gordeliy VI, Kiselev MA, Lesieur P, Pole AV, Teixeira J (1998) Lipid membrane structure and interactions in dimethyl sulfoxide/water mixtures. *Biophys J* 75(5): 2343–2351.
18. Chang HH, Dea PK (2001) Insights into the dynamics of DMSO in phosphatidylcholine bilayers. *Biophys Chem* 94(1-2):33–40.
19. Franck JM, Pavlova A, Scott JA, Han S (2013) Quantitative cw Overhauser effect dynamic nuclear polarization for the analysis of local water dynamics. *Prog Nucl Magn Reson Spectrosc* 74:33–56.
20. Cheng C, Song J, Pas J, Meijer L, Han S (2015) DMSO induces dehydration near lipid membrane surfaces. *Biophys J* 109(2):330–339.
21. Donaldson SH, Jr, et al. (2015) Developing a general interaction potential for hydrophobic and hydrophilic interactions. *Langmuir* 31(7):2051–2064.
22. McIntosh TJ, Simon SA (1993) Contributions of hydration and steric (entropic) pressures to the interactions between phosphatidylcholine bilayers: Experiments with the subgel phase. *Biochemistry* 32(32):8374–8384.
23. Israelachvili JN, Wennerström H (1990) Hydration or steric forces between amphiphilic surfaces? *Langmuir* 6(16):873–876.
24. LeNeveu DM, Rand RP (1977) Measurement and modification of forces between lecithin bilayers. *Biophys J* 18(2):209–230.
25. Israelachvili JN, Wennerström H (1992) Entropic forces between amphiphilic surfaces in liquids. *J Phys Chem* 96(2):520–531.
26. Israelachvili J, et al. (2010) Recent advances in the surface forces apparatus (SFA) technique. *Rep Prog Phys* 73(3):1–16.
27. Israelachvili JN (2011) *Intermolecular and Surface Forces* (Elsevier, San Diego), 3rd Ed.
28. Marra J, Israelachvili J (1985) Direct measurements of forces between phosphatidylcholine and phosphatidylethanolamine bilayers in aqueous electrolyte solutions. *Biochemistry* 24(17):4608–4618.
29. Pincet F, Perez E, Wolfe J (1994) Do trehalose and dimethyl sulfoxide affect intermembrane forces? *Cryobiology* 31(6):531–539.
30. Kuhl TL, Leckband DE, Lasic DD, Israelachvili JN (1994) Modulation of interaction forces between bilayers exposing short-chained ethylene oxide headgroups. *Biophys J* 66(5):1479–1488.
31. Pincet F, Cribier S, Perez E (1999) Bilayers of neutral lipids bear a small but significant charge. *Eur Phys J B* 11(1):127–130.
32. Hemmerle A, et al. (2012) Controlling interactions in supported bilayers from weak electrostatic repulsion to high osmotic pressure. *Proc Natl Acad Sci USA* 109(49): 19938–19942.
33. Claesson PM, Kjellander R, Stenius P, Christenson HK (1986) Direct measurement of temperature-dependent interactions between non-ionic surfactant layers. *J Chem Soc Faraday Trans 1* 82(9):2735–2746.
34. De L, Costello BA, Luckham PF, Tadros ThF (1993) Forces between adsorbed low molecular weight graft copolymers. *J Colloid Interface Sci* 156(1):72–77.
35. McIntosh TJ, Simon SA (1986) Hydration force and bilayer deformation: A reevaluation. *Biochemistry* 25(14):4058–4066.
36. Stejskal EO, Tanner JE (1965) Spin diffusion measurements: Spin echoes in the presence of a time-dependent field gradient. *J Chem Phys* 42(1):288–292.
37. Pashley RM (1981) DLVO and hydration forces between mica surfaces in Li^+, Na^+, K^+, and Cs^+ electrolyte solutions: A correlation of double-layer and hydration forces with surface cation exchange properties. *J Colloid Interface Sci* 83(2):531–546.
38. Pacak P (1987) Polarizability and molecular radius of dimethyl sulfoxide and dimethylformamide from refractive index data. *J Solution Chem* 16(1):71–77.
39. Schneck E, Sedlmeier F, Netz RR (2012) Hydration repulsion between biomembranes results from an interplay of dehydration and depolarization. *Proc Natl Acad Sci USA* 109(36):14405–14409.
40. Bunton CA, Mhala MM, Oldham KG, Vernon CA (1960) The reactions of organic phosphates. Part III. The hydrolysis of dimethyl phosphate. *J Chem Soc* 0:3293–3301.
41. Pelta MD, Morris GA, Stchedroff MJ, Hammond SJ (2002) A one-shot sequence for high-resolution diffusion-ordered spectroscopy. *Magn Reson Chem* 40(13):S147–S152.
42. Chen HC, Chen SH (1984) Diffusion of crown ethers in alcohols. *J Phys Chem* 88(21): 5118–5121.
43. Kuhl T, et al. (1996) Direct measurement of polyethylene glycol induced depletion attraction between lipid bilayers. *Langmuir* 12(12):3003–3014.
44. Sacco A, Matteoli E (1997) Isotopic substitution effects on the volumetric and viscosimetric properties of water-dimethylsulfoxide mixtures at 25° C. *J Solution Chem* 26(5):527–535.
45. Pashley RM (1981) Hydration forces between mica surfaces in aqueous electrolyte solutions. *J Colloid Interface Sci* 80(1):153–162.
46. Pashley RM, Israelachvili JN (1984) Molecular layering of water in thin films between mica surfaces and its relation to hydration forces. *J Colloid Interface Sci* 101(2): 511–523.
47. Parsegian VA, Gingell D (1972) On the electrostatic interaction across a salt solution between two bodies bearing unequal charges. *Biophys J* 12(9):1192–1204.
48. McDaniel RV, McIntosh TJ, Simon SA (1983) Nonelectrolyte substitution for water in phosphatidylcholine bilayers. *Biochim Biophys Acta* 731(1):97–108.
49. Kaatze U, Pottel R, Schäfer M (1989) Dielectric spectrum of dimethyl sulfoxide/water mixtures as a function of composition. *J Phys Chem* 93(14):5623–5627.
50. Catalán J, Díaz C, García-Blanco F (2001) Characterization of binary solvent mixtures of DMSO with water and other cosolvents. *J Org Chem* 66(17):5846–5852.